



Interpretation of Gravity Monitoring Data on Geotechnical Impact on the Geological Environment

SERGEY BYCHKOV,¹  ALEXANDER DOLGAL,¹ and ALEXEY SIMANOV¹

Abstract—The Verkhnekamskoye potassium salt deposit located in the Perm Krai is the main source of raw materials for the potash industry in Russia. The penetration of underground waters into the shafts of the mine, which is situated beneath the industrial zone, and residential quarters of the city of Berezniki led to the flooding of the mine with subsequent collapsing of the earth's surface. For obtaining the information about negative impacts of engineering processes associated with mineral mining operations, a method of highly accurate gravimetric monitoring observations is suggested, suitable for tracking the time changes of the gravitational field. As a result of monitoring observations we obtain a dynamic anomaly of gravity which is defined as the difference between the subsequent and the previous gravity values. Since all the unvarying components of the gravitational field are present in each pair of the observations, the dynamic anomaly only reflects a specific geological or mining process. The method for processing and interpretation of the dynamic anomalies of gravity, which synthesizes qualitative and quantitative approaches to extracting the geological information from gravity data, is developed. The interpretation yields the areal distribution and probable depth interval of the zone of rock decompaction and shows the magnitude of the change in the density of rocks characterizing the intensity of the decompaction process. The practical implementation of the highly accurate gravimetric monitoring observations is carried out in the emergency sites of the mines of the Verkhnekamskoye potassium salt deposit has demonstrated high efficiency of the suggested method.

Keywords: Gravity monitoring, numerical modeling, induced subsidence, salt mine, safety control.

1. Introduction

Long-term manmade loads associated with the production activities at mineral deposits can have a strong impact on the natural geological environment. These impacts can cause a response in the form of the

large-scale changes leading to the catastrophic consequences such as subsidence and collapsing of the earth's surface which threaten the life activities and are fraught with the significant economic losses (Ogilvy and Bogoslovsky 1979; Branston and Styles 2003; Baryakh et al. 2011; Strzałkowski 2019; Con-trucci et al. 2019). The study and forecast of the negative impact of engineering processes on the geological environment is widely based on the combined use of geophysical methods, among which gravity plays an important role (Arzi 1975; Rybakov et al. 2001; Pinto et al. 2005; Branston and Styles 2003; Styles et al. 2006; Pringle et al. 2012; Sultan and Ahmed 2014; Zong et al. 2015; Constantino et al. 2016; Nava-Flores et al. 2016; Santolaria et al. 2017; Gabriel et al., 2019; Tsiupiak et al. 2019). The critical importance of identifying the technological impact on the geological environment is demonstrated, inter alia, by the recent catastrophic accidents with flooding of the mines of the Verkhnekamskoe potash deposit (VKPD).

This potassium salt field located in the Perm Krai (Fig. 1) is the main source of raw materials for the potash industry in Russia. Tectonically, it is confined to the central part of the Solikamsk depression of the Cis-Uralian foredeep (Fig. 1). The deposit is a lens-shaped Kungurian salt stratum up to 550 m thick with an area of more than 8000 km². The depth to the top of the salt layer varies from 150 to 700 m. The potash field mainly composed of carnallite and sylvinite is located within the boundaries of the halite stratum. Much attention has always been paid to studying the geological structure of the deposit and its safe development (Baryakh et al. 2011; Kovin 2011).

For detecting the gravity variations associated with the human impact on the geological

¹ Mining Institute of Ural Branch of Russian Academy of Science, str. Sibirskaya, Perm, Russia 78A 614007. E-mail: bsg@mi-perm.ru

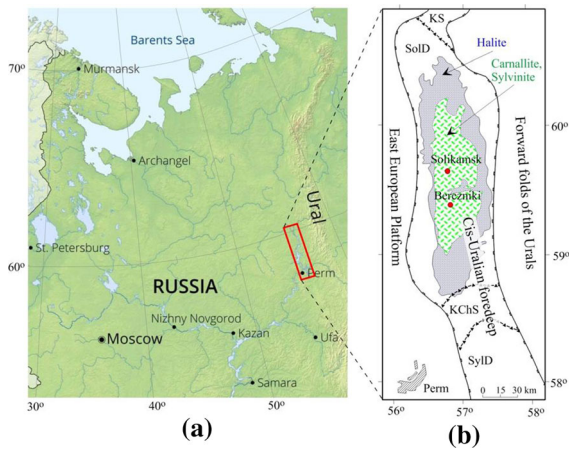


Figure 1

Verkhnekamskoye potassium salt deposit in the Perm Krai: **a** geographical location, **b** tectonic framework (KS–Kolvinskaya Saddle, SolD–Solikamskaya Depression, KChS–Kosvinsko-Chusovskaya Saddle, Sylvenskaya Depression)

environment, the time-lapse monitoring gravity observations are carried out at VKPD (Shcherbinina et al. 2011; Bychkov et al. 2018b). The monitoring observations of gravity reveal the dynamics of the deformation processes of the rock mass and make it possible to forecast dangerous and catastrophic situations. The time-lapse observations are used for calculating the dynamic anomaly of gravity which is defined as the difference between the subsequent and previous gravity values. Dynamic anomalies are not distorted by the terrain effects and do not reflect the time-constant density inhomogeneities of the geological section. Since all the constant components of the gravitational field are equally present in any pair of the observations, the dynamic anomaly only reflects a specific mining process or a rapid geological process occurring on a certain time interval.

Gravity monitoring is widely used in the studies of volcanic activity and in hydrogeology (Jentzsch et al. 2004; Carbone and Greco 2007; Biegert et al. 2008). The use of gravity data is highly efficient in studying the karst phenomena (Rybakov et al. 2001; Eppelbaum et al. 2008; Jacob et al. 2009; Al-Zoubi et al. 2013). Extensive monitoring observations are carried out at the oil and gas fields where gravity data are used for determining the changes in the reservoir pressure and for estimating the rise of the oil- and gas-water contact (Gelderen et al. 1999; Glegola et al.

2015; Reitz et al. 2015) as well as for controlling the CO₂ injection into the reservoir aimed at enhancing oil recovery of the fields (Gasperiakova and Hoversten 2008). The studies of the earth's surface subsidence and the development of underground cavities above salt mines from gravity data are carried out in the UK (Branston and Styles 2003; Styles et al. 2006; Pringle et al. 2012) and Ukraine (Tsiupiak et al. 2019).

The geological efficiency of the geophysical and, in particular, gravimetric studies significantly depends on the interpretation technologies, which include various methods for extracting information from field observations. The interpretation methods are traditionally divided into qualitative and quantitative (Jacoby and Smilde 2009). Qualitative interpretation approximately estimates the spatial distribution of density inhomogeneities corresponding to the revealed gravity anomalies. Quantitative interpretation yields the parameters characterizing the anomalous geological objects, namely, their shape, size, depth, density, etc. We propose a variant of the synthesis of qualitative and quantitative methods for extracting geological information from gravimetric data, which, in our opinion, improves the reliability of locating the anomalous objects.

2. Geological Model of Gravimetric Monitoring

Since dynamic anomalies do not reflect static density inhomogeneities present in the geological section, the model of gravimetric monitoring consists of a homogeneous geological medium hosting an isolated domain where the density of rocks has changed. For example, in the geological section shown in Fig. 2a, a decompacted zone with a density σ_3 appeared (let us say, a karst cavity) (Fig. 2b). The gravity field has slightly decreased; however, it is very difficult to identify this geological object with only the field Δg_{T2} . If we calculate the difference $\delta g = \Delta g_{T2} - \Delta g_{T1}$, then we get only the gravitational effect of the decompressed zone (Fig. 2c). The extreme magnitudes of the gravitational effects depending on the depth (H) and size (R) of the decompaction zone are shown by the curves in Fig. 2d (the values are indicated in mGal). These effects are calculated for the case when the density of the local object changes by 10 kg/m³, which

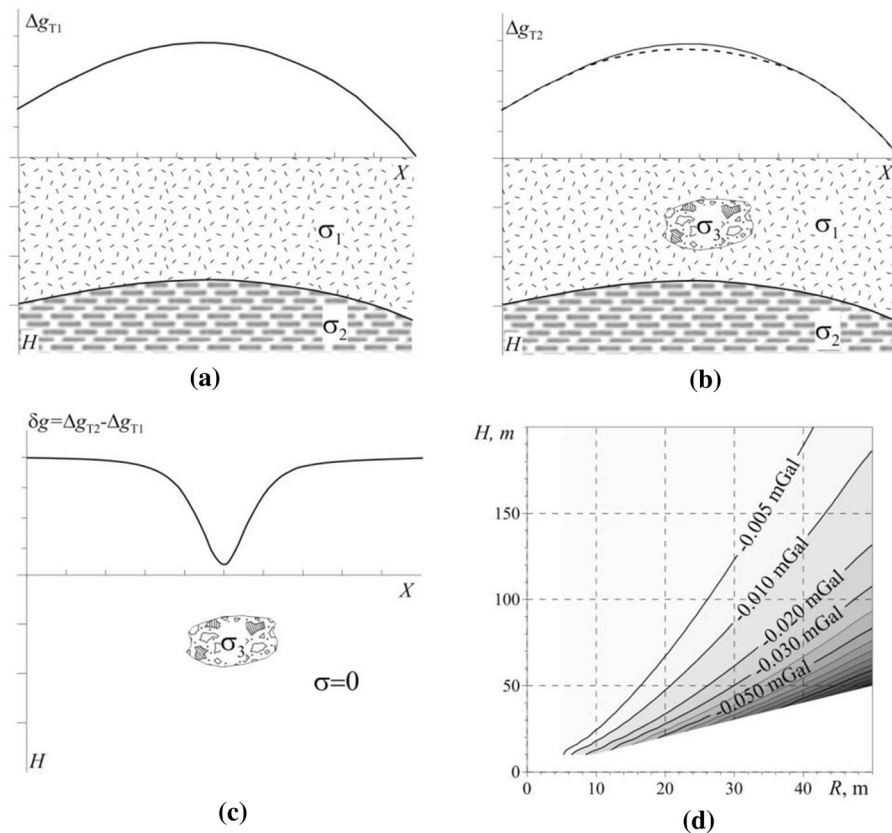


Figure 2

Geological model of gravity monitoring: **a** gravity field Δg_{T1} of a two-layer geological model with densities σ_1 and σ_2 (scales along the axes are conventional), **b** gravity field Δg_{T2} with a zone of decompression σ_3 (dashed line), **c** dynamic gravity anomaly, **d** extreme gravitational effects of the models depending on depth (H) and dimensions (R) of the anomalous bodies

is a very small value. Due to the fact that modern gravimetric and geodesic instruments detect gravity anomalies as accurately as up to $\pm(0.005\text{--}0.007)$ mGal (Chapin et al. 1999), based on the gravimetric data it is possible to determine the beginning of the process of rock decompression by identifying the zones of the probable subsequent subsidence and collapsing of the earth's surface.

There are several noise components in gravimetric monitoring: changes in the elevation of an observation point, in the thickness and density of the snow cover, variations in the atmospheric pressure, seasonal changes in water saturation and in the degree of frost penetration in the upper part of the section, the groundwater level in the vicinity of the observation point, and some other factors. The external factors of the changes in gravity field which

include tidal effect, the changes in the local landforms in the vicinity of the observation point (man-made dumps, ditches, etc.), and variations in the atmospheric pressure, can be taken into account during data processing (Al-Zoubi et al. 2013). The endogenous factors and, primarily, the groundwater level which noticeably affects the gravity field as demonstrated in (Davis et al. 2008; Jacob et al. 2009; Gabriel et al. 2019) are more difficult to take into account. Clearly, for each segment of the gravimetric works, the relationship between the fluctuations of the groundwater level and the changes in gravity will be different; therefore, monitoring should be accompanied by gravimetric observations at the existing hydrogeological wells with tracking the groundwater level and identifying the relationship between its fluctuations and the changes in gravity.

Based on the suggested model of gravimetric monitoring and considering the world experience in the gravimetric monitoring studies, we developed a technique for the joint application of the qualitative and quantitative interpretation methods. At the initial stage of the interpretation, the image of the geological medium (3D field model) is constructed by the tomographic transformation of the field. The depth scale of the constructed cross sections and 3D diagrams of the field does not correspond to the true one and is graduated in the transformation coefficients (k). However, the results of the tomographic transformation are successfully used for refining the geological hypotheses and for specifying the a priori constraints in the subsequent solution of the gravity inversion.

We propose to solve the inverse problems by the assembly method with the use of the guaranteed approach to assessing the quality of the obtained results and with constructing the localization function of the anomalous bodies. The idea of the assembly method is to assemble the anomalous object by attaching an elementary volume to the initial model in such a way that the difference between the measured and model field decreased at each step of the iteration process. The method uses a discrete (grid) description of a density medium where the anomalous objects are represented in the form of an aggregate of a certain number of elementary geometric bodies (for example, cubes). By varying the parameters of transformations of the field, we obtain different sets of the constraints on the parameters of the anomalous bodies. Multiple solutions of the inverse problem for each model yield different shapes and different locations of the objects. Combining all the solutions, we obtain a domain, which is guaranteed to contain the anomalous objects, and a domain where these objects can be located with a certain degree of reliability. The model of the field's source used in this method (isolated objects in a homogeneous environment) fully satisfies the geological model of gravimetric monitoring since the effect of the constant density inhomogeneities associated with the geological structure of the rock mass is absent in the dynamic gravity anomalies.

3. Qualitative Interpretation of Dynamic Anomalies

At present, numerous algorithms have been developed for constructing three-dimensional models of various parameters (characteristics) of the potential fields for spatial mapping of the geological medium, and a new direction called interpretation tomography has been formed in the theory of interpretation of the potential fields (Mauriello and Patella 2001; Bychkov et al. 2003; Novoselitskiy et al. 2003; Prostolupov et al. 2006; Chianese and Lapenna 2007; Sailhac et al. 2009; Dolgal et al. 2012; Florio and Fedi 2014; Liu et al. 2014; Xiao 2015; Bychkov 2018 a, b). The methods of interpretation tomography are very attractive for geophysicists because these methods allow the interpreted field to be separated into the contributions of the layers located at the different depths with a minimum a priori information about the anomalous bodies; they do not require burdensome procedures for constructing the initial approximation (geological models) which are necessary in the classical methods of automated fitting of the field, and they use relatively fast computational algorithms that allow processing large amounts of the initial information.

One of the methods of tomographic interpretation is vector scanning which is implemented in the VECTOR computer technology, described in works (Bychkov et al. 2003; Novoselitskiy et al. 2003; Prostolupov et al. 2006; Shcherbinina et al. 2011). At the initial stage of processing in the VECTOR system, triangulation is carried out over the irregular grid of the points distributed in area D : $x_1 \leq x \leq x_2$, $y_1 \leq y \leq y_2$, at which the analyzed field V was measured (the Bouguer anomalies). This procedure yields a system of the multiple overlapping triangles at the intersections of the medians of which the orthogonal components V_x and V_y of the horizontal gradient are stably determined. The vertices of the triangles are the observation points. The system of the triangles is dense and multiply overlapped. In each triangle, the orthogonal components V_x and total vector of horizontal gradient $V_s = V_x + V_y$ are determined from three increments of the field. The horizontal gradients whose bases lie at intersections of medians of a triangle are the initial and main material for the subsequent transformations of the field in a system of

vector transforms (Prostolupov et al. 2006). Here, by varying the constraints on the triangulation process (primarily, the equilaterality condition for the triangles), we can obtain different variants of the solution.

Next, vector averaging of the gradients (with vector directions taken into account) is carried out in the moving windows of various sizes L^1, L^2, \dots, L^N and the background field component is removed. The window size is increased with a given step from the minimal value, which is equal to the average length of the side of a triangle to the maximal value, which is equal to the size of the study area. The calculation of the differences \mathbf{V}_x^k and \mathbf{V}_y^k between the gradients of the original field and their averaged values yields local components. The values of the local field are calculated by the numerical integration of the obtained discrete values: $\mathbf{V}^k = \iint_D \mathbf{V}_s^k dx dy$.

The obtained results - field components V^1, V^2, \dots, V^N - are identified with the anomalous effects caused by the fragments of the geological environment that are bounded by the earth's surface and by some consistently increasing effective depths $h_{ef}^1, h_{ef}^2, \dots, h_{ef}^N$ with the allowance for the fact that the size of the anomaly for the same geological object depend on the depth to this object. Respectively, the field component ΔV^k reflecting the contribution of the k th horizontal layer whose top is located at the depth h_{ef}^{k-1} and the bottom at the depth h_{ef}^k is determined by formula $\Delta V^k = V^k - V^{k-1}$. The behavior of function ΔV^k is strongly related to density distribution within the k th layer and, hence, it can be used for detecting and delineating the anomalous geological objects located in a certain depth interval. It is possible to construct a three-dimensional diagram of the field $\sum_{k=1}^N \Delta V^k$ and various sections of this diagram by 3D interpolation of the fields V^1, V^2, \dots, V^N (Bychkov et al. 2003; Novoselitskiy et al. 2003). The z -axis in the 3D field diagrams is scaled in the units of transformation ratio - the area ratio of the moving window to the study region.

The effect of identifying different depth field sources during vector scanning is resulting from the different nature of the field decrease with distance from the field source and its gradient. Since the gradient decreases noticeably faster whereas averaging in the moving window takes into account the direction of the gradient vector, the effect of the near-

surface anomalous bodies is much stronger suppressed by the integration over a large area than by the traditional averaging of the field in the moving window.

The diversity of the options to vary the size and shape of the moving window as well as the fairly vague correlation between the window size and effective depths does not allow for strict determination of the geometrical parameters of the geological objects. However, the results of processing by the VECTOR system can be used, for example, as the zero-approximation model for preliminary estimating the structural and tectonic features and for comparing gravity data with other geological and geophysical information (Bychkov 2018a, b). By varying the parameters of the transformations, we obtain different sets of the a priori data for solving the inverse problem.

4. The Solution of the Nonlinear Inverse Problem in Gravimetry

The parameters characterizing the shape, the size, and the depth of the anomaly-forming objects make it possible to obtain the solution of the nonlinear inverse problem. This can be fairly efficiently done by the assembly algorithm which implements the finite-element approach to gravity modeling proposed by Strakhov and Lapina (1976) and which was further developed in the works of Balk and Dolgal (2009, 2010, 2014, 2018) and Balk et al. (2012). The method uses a discrete (grid) description of a density medium where the anomalous objects (configurations) Ω are represented in the form of an aggregate of a certain number of elementary geometric bodies (for example, cubes) whose density is assumed to be constant (Camacho et al. 2000; Balk and Dolgal 2009). Each anomalous object is "assembled" from fairly small (equal to grid size) elements ω_x . Here, at each i -th step of the iterative process, the core of the current configuration Ω_i is augmented by one element ω_x , that provides the smallest root mean square residual ε between the observed and the model fields. At the transition from configuration Ω_i to configuration Ω_{i+1} , the main a priori information that the interpreter usually has about the location, the shape,

and size of the anomalous bodies is taken into account. As the volume of the anomalous body grows, its density decreases. The density is one of the optimizable parameters and can be specified in the form of the interval estimate (Balk et al. 2012). When the anomalous body achieves the a priori prescribed value of density by the source, the process of solving the inverse problem is stops.

The finite-element approach to solving the inverse problem removes the problem of instability in its classical sense because the finite dimension of the model and the natural constraints on its density and geometric parameters a priori lead to the compact set of the probable solutions whereas the allowance for a certain set of the a priori information in constructing the effective configurations yields a reliable solution of a geological problem under consideration. The necessary a priori constraints specified by the interpreter include the number and densities of the bodies in the model of the anomalous domain; the position of the fragments of each body (at least one element ω_x for each body); the permissible value of the residual between the original and the fitted fields (typically, in the Euclidean metric); and the side length of the cubic element of the tessellation ω_x . The following information is optional (but desirable for improving the reliability of the interpretation results): the domain that surely contains anomalous bodies; the domain that is known not to contain anomalous bodies; the minimum and maximum probable depths of the top and bottom edges of the bodies; the constraints on the vertical and horizontal thickness of each body; any fragments of bodies (besides the necessary ones); the admissibility conditions for the contact between the individual anomalous bodies; the condition of smoothness of the surfaces of the bodies.

As a rule, interpretation considers an individual solution of the inverse problem, which is a point estimate of model parameters. This solution always contains random peculiarities. To increase the reliability of interpretational constructions, it is advisable to analyze the entire reliable information about the disturbing objects that is contained in the measurements of the field. The methodology for building these constructions is based on the guaranteed approach, which was developed in relation to gravity in (Balk and Dolgal 2010). This approach is aimed at

extracting information in the conditions of uncertainty and has proven to be efficient in many fields of science, primarily in the control theory (Chernousko 1981; Bakan 2000).

For this purpose, it is necessary to form a representative set of the feasible solutions of the inverse problem, i.e. the interpretation models that provide the required value of the residual ε between the observed and model fields and satisfy the existing a priori constraints on the parameters of the anomalous bodies. We note that all the solutions included in this set should differ by at least one element. The problem of localizing a single perturbing body can now be considered as the problem of constructing a pair of the domains in the studied volume of the medium: domain D_1 containing all the feasible solutions of the inverse problem and domain D_2 which is a fragment of all the feasible solutions (and, hence, also a fragment of the anomalous object itself).

In terms of the set theory, the union of all the solutions contained in the set that we have formed is the domain D_1 , and the intersection of the solutions is the domain D_2 (Balk and Dolgal 2010). In this case, domain $D_1 \setminus D_2$ of the geological medium is the region of uncertainty whose Lebesgue measure μ gives a quantitative estimate of the practical equivalence for a given inverse problem whereas the extension of the metric $\tau(D_1, D_2) = 1 - \mu(D_2) / \mu(D_1)$ is an estimate of the informativity of the aggregate data. To clarify on this, in the case of solving a 3D inverse gravimetric problem, measure μ is the volume ratio of domains D_1 and D_2 , while in the case of solving a 2D inverse gravimetric problem, this measure is the area ratio of these domains. However, the guaranteed approach in its “pure form” is, in a sense, excessively categorical - when solving many practical problems, it becomes impossible to construct the area D_2 . For example, among the 500 feasible solutions of the inverse problem in the sample, only 499 solutions intersect with each other. The existence of only one solution, the most different from the others, leads to the situation $D_2 = \emptyset$. In this case, it is advisable to switch to spatially probabilistic estimates.

Let us illustrate the guaranteed approach by a model example. Consider the anomaly of the gravitational field created by three prisms with anomalous densities 200, 300, and 500 kg/m³ (Fig. 3). The

“observed” field was obtained by solving the direct gravimetric problem and its amplitude varies from 2.57 to 19.46 mGal. The solutions of the inverse problem in which the rms residual is within 0.2 mGal (i.e., below 1% of the maximum gravity value) were considered feasible. The a priori information included the following quantitative constraints: the depth to the bottom edges of the anomalous bodies is at most 10 km; the horizontal width of the bodies is at most 10 km, and the vertical thicknesses are 4, 4, and 2 km, respectively. The qualitative constraints are following: the boundary of each perturbing object is quite smooth and the anomalous bodies can be in pairwise contact. Elements ω_α are prisms 0.25×0.25 km square section. With the use of the assembly method with exact density values, 241 feasible solutions of the inverse problem were found. All these solutions lie within domain D_1 covering about 36% of the area of the modeled section; domains D_2 are relatively small. Moreover, in the case of the deepest body no. 2, domain D_2 is absent, i.e. under given conditions; any fragment of this body cannot be identified with guarantee by solving the inverse problem even if the noise level in the “observed” field is relatively low: $\delta_z = 0.2$ mGal.

It appears more efficient to rank the studied volume of the medium according to the probability of the presence of the sought anomalous objects. The principle of this ranking is following: since all the feasible solutions of the inverse problem are a priori peer, each of them may equally probably be the best approximation of the unknown perturbing object Ω . We denote the number of all the feasible solutions of

the inverse problem that are contained in the set ($N \approx 10^2 - 10^3$) by N and the number of the feasible solutions Ω_k^* where k is the number of the solution, each of which contains a specific element ω_α by $N_{k,\alpha}$. Then $p_{k,\alpha} = N_{k,\alpha}/N$ is the estimate of the probability that this element ω_α is a small fragment of the sought perturbing object Ω . Hereinafter, this estimate will be referred to as the localization function: $p_{k,\alpha} = p_{k,\alpha}(x,y,z)$, where x,y,z are the coordinates of the center of gravity of element ω_α . The spatial distribution of the localization function, in contrast to any partial solution of the inverse problem, makes it possible to identify the common, regular features of the geometric parameters of anomalous objects, i.e. to reduce the manifestation of ε -equivalence (Balk and Dolgal 2014, 2018) or, in other words, practical ambiguity of the solution of the inverse gravimetric problems.

5. Synthesis of the Methods of Qualitative and Quantitative Interpretation

The necessary information for solving the inverse problem can be obtained by the method of interpretation tomography (Bychkov et al. 2013; 2018a). The anomalous zones ϑ that were revealed by the interpretation tomography and which can be identified, in the first approximation, with the disturbing objects under study contain elements ω_α (“crystallization centers”), one element per each modeled source. Elements ω_α are randomly distributed within these zones. The locations of these elements are generated similarly to how it is done in the Monte Carlo method, in the form of a multidimensional parameter vector $\mathbf{P} = \{p_1, p_2, \dots, p_m\}$ where $p_i = (x_i, y_i, z_i)$ are the Cartesian coordinates of the unique element ω_α that pertains to the i -th perturbing object and m is the number of sources. Here, it is implied that the distribution of the points p_i within the corresponding anomalous zones ϑ_i , $i = 1, 2, \dots, m$, is uniform. The inverse problem is then repeatedly solved (with $\sim 10^2 - 10^3$ repetition cycles) by the assembly method, and the resulting set of the partial solutions is transformed into the localization function - the grid distribution of the probability characteristics $p_{k,\alpha}(x,y,z)$ which is an informative statistical model of

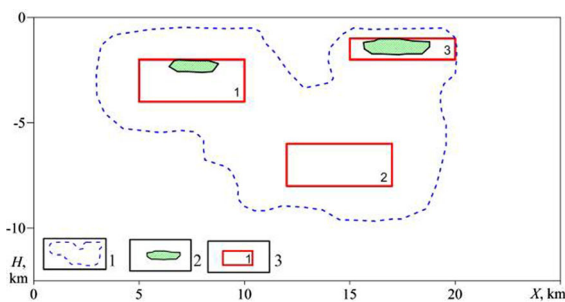


Figure 3

Implementation of the guaranteed approach to solving the inverse problem of gravity: (1) contour of domain D_1 ; (2) contour of domain D_2 ; (3) anomalous prisms and their numbers

rock density. In contrast to the results of interpretation tomography, this model has the real spatial coordinates x , y , z and characterizes the distribution of anomalous masses within the studied volume of the geological medium from the standpoint of probability theory. As is evident, the value of the localization function is the estimate of geometrical probability that elements ω_x pertain to the sought anomalous objects. The domains of high values of parameter $p_{k,z}$ correspond to the most reliably identified fragments of the anomalous objects, which can then be used for planning the locations of the boreholes or mine workings.

However, it is not possible to relate strictly these domains to the boundaries of the anomalous objects as the former are the characteristics reflecting the structure of the set of the feasible solutions of the inverse problem and, in the general case, they do not provide the required closeness between the observed and model fields. For localizing the anomalous bodies, it is necessary to select one “best” particular solution of the inverse problem. This can be done with the use of various criteria. We note that unlike the theoretical situations, achieving the minimum residual between the observed and model fields in the conditions of unremovable (geological) noise with unknown distribution law does not entail the best spatial coincidence between the real and model density heterogeneities. One of the criteria for selecting a particular solution of the inverse problem is the criterion of the maximum a posteriori probability P_{\max} according to which it is assumed that the true distribution of mass is fitted best by the solution consisting of a set of elements ω_x that satisfies the condition $(\sum p_{k,z})/N_{k,z} = \max$, where $N_{k,z}$ is the number of elements in this solution.

Let us return to the model example shown in Fig. 3 where gravity anomalies are produced by three infinite-length horizontal prisms. The gravitational field of these prisms, which is depicted in the upper part of Fig. 4, does not clearly suggest the presence of three anomalous bodies in the section. The tomographic transformation of this field in the VECTOR system allows the separation of the total gravitational effect and construction of the first-approximation model for solving the inverse problem of gravity, which consists of three bodies.

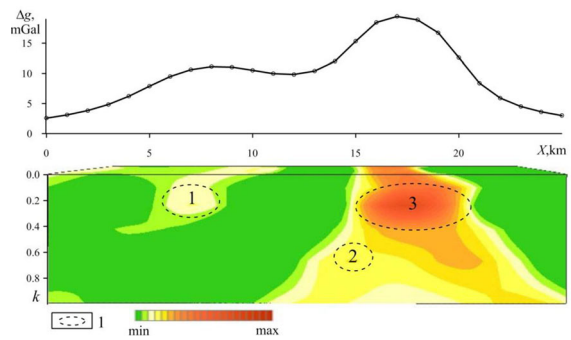


Figure 4

Gravity field and vertical cross section of the 3D diagram of the field created (in conventional units) by three prisms: (1) anomalous zones ϑ corresponding to the anomalous bodies

The set of the solutions of the inverse problem (overall, a total of $N = 241$ finite-element feasible models satisfying the condition $\varepsilon \leq 0.2$ mGal were constructed) for this model of the medium is characterized by the localization function (Fig. 5a). Clearly, the particular solution of problem corresponding to the criterion of the maximum a posteriori probability P_{\max} with a residual of 0.185 mGal (Fig. 5b) more accurately localizes the true anomalous bodies than solution which provides the minimum residual 0.141 mGal between the observed and model fields (Fig. 5c).

6. Gravity Monitoring at the Emergency Sites of Potash Mines

Let us demonstrate the suggested interpretation method by the example of gravity monitoring observations of the VKPD minefields. In 2006, the penetration of underground waters into the shafts of the mine, which is located beneath the industrial zone, and residential quarters of the city of Berezniki led to the flooding of the mine with subsequent collapsing of the earth's surface. In the region of the sinkholes, the detailed gravity monitoring surveys were carried for delineating and studying the dangerous zones, establishing their nature, determining the depth limit of rock decompaction, and identifying the potentially dangerous segments in the neighboring territories.

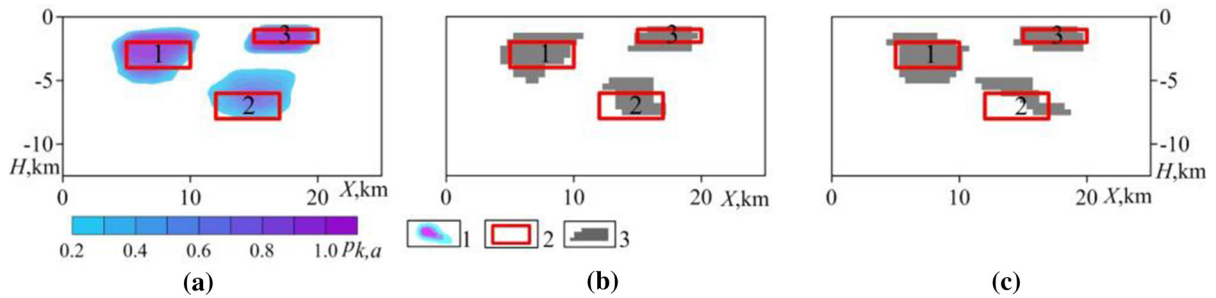


Figure 5

Results of solving the inverse problem of gravity with the use of assembly algorithm: **a** localization function $p_{k,a}$; partial solutions corresponding to the criterion of the **b** maximum a posteriori probability and **c** minimum residual of the fields; (1) contours of the equal $p_{k,a}$ values; (2) anomaly-forming prisms; (3) the fitted anomalous objects.

Figure 6 shows the Bouguer anomaly for the gravity field measured in November 2010 after the sinking of the earth's surface whose contour is denoted by number I. In this area, several cycles of gravity measurements have been carried out. In February 2011, the survey was repeated over the entire area; in September 2011 in the central part and in 2016–2018, in the eastern part of the territory.

Gravity measurements were carried out at the fixed metalmarks (dowels hammered into asphalt) on 50×50 m grid by the AUTOGRAV CG-5 gravimeters. A differential GPS Trimble R-8 GNSS receiver performed height and plan positioning of gravity stations. The determination accuracy of the observed gravity field and elevations of survey points was ± 0.005 – 0.010 mGal and ± 0.01 – 0.02 m, respectively. Independent observations were repeated at each point until the required accuracy was achieved. Observations were taken relative to the

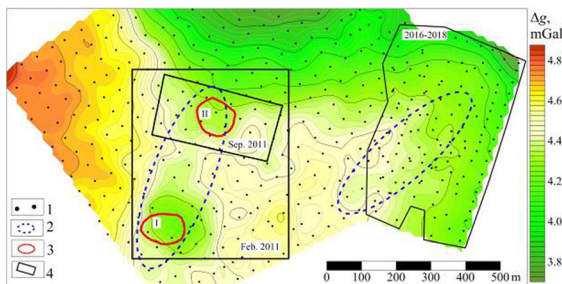


Figure 6

The Bouguer gravity anomaly in the region of surface subsidence: (1) gravity stations; (2) local negative gravity anomalies; (3) sinkholes (I, November 2010; II, December 2011); (4) areas of time-lapse gravity survey

initial gravimetric point, which is located 15 km away from the city outside the zone affected by geotechnical, mining, and geodynamic processes. The comparison was conducted for the Bouguer anomalies, i.e. the changes in the heights of gravity stations were taken into account. Considering the relatively small size of the studied territory, we believe that the ground water level whose variations may lead to the change in gravity varied synchronously throughout the study area. Such variations could lead to the change in the overall field level without generating local anomalies.

The repeated survey in February 2011 revealed dynamic gravity anomalies with amplitudes up to -0.15 mGal only close to sinkhole I (Fig. 7a). A remarkable feature is that the dynamic anomaly spatially coincides with the local negative gravity anomaly (Fig. 7b). This can be interpreted as the existence of a natural zone of decompacted rocks, which is related to the technogenic karst processes leading to the collapses of the land surface. The interpretation results of the dynamic anomaly in the VECTOR system (Fig. 7c) and the constructed localization function (P) (Fig. 7d) have shown that the decompaction zone is located at the depth H from 50 to 100 m and confined to the water resistant impermeable suprasalt stratum whose collapse has resulted in the formation of the sinkhole.

The time-lapse gravimetric measurements in the zone of intense surface subsidence north of the sinkhole were repeated in September 2011. These measurements revealed a dynamic gravity anomaly (Fig. 8) testifying to the process of rock

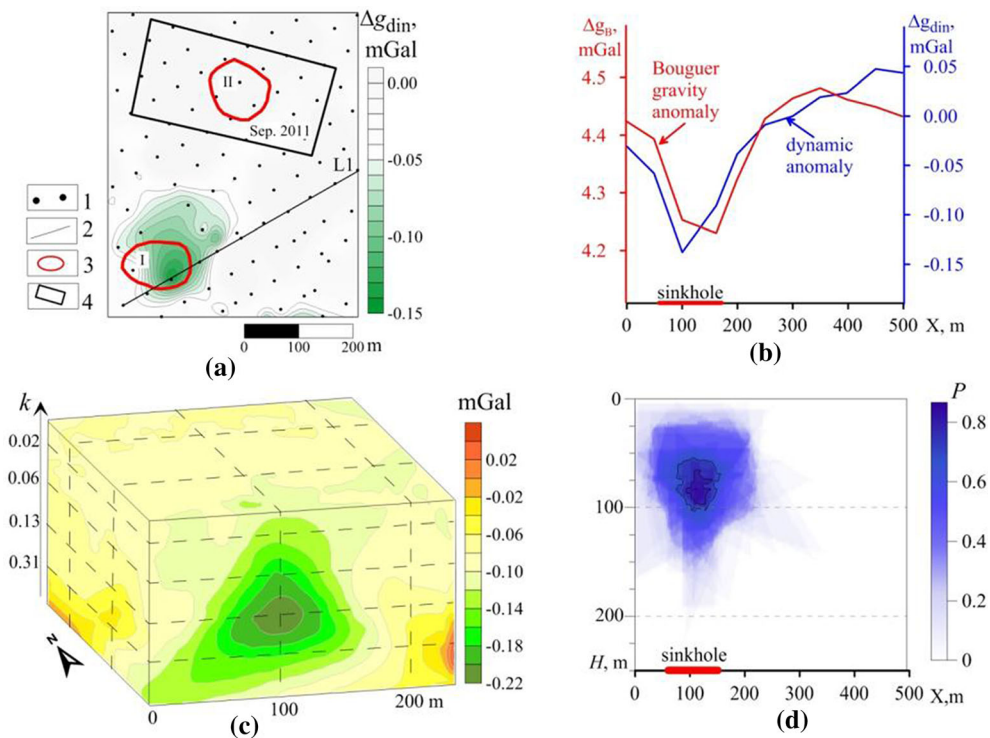


Figure 7

Interpretation results of monitoring observations in the region of sinkhole I: **a** dynamic gravity anomalies over period from November 2010 to February 2011: (1) gravity stations; (2) L1 profile line; (3) contours of sinkholes; (4) survey area in September 2011; **b** graphs of the Bouguer anomalies and the dynamic anomaly on profile L1; **c** local anomaly identification in VECTOR system; **d** cross section of the localization function



Figure 8

The dynamic gravity anomaly (September to February 2011) against the urban terrain: (1) gravity stations; (2) contour of surface subsidence in December 2011

decompaction that had begun after February 2011. The further development resulted in the formation of another sinkhole in December 2011 (denoted by

number II in Figs. 6 and 7a) within the revealed zone of the north striking negative local gravity anomalies revealed by the survey in September 2011. By 2014, a technogenic lake (Fig. 9) had formed at the location of these sinkholes. The strike of this lake was determined by the local negative Bouguer anomaly (Fig. 6).

In 2016–2018, gravimetric measurements were continued in the eastern part of this territory (Figs. 10 and 11). Over the period from September to December 2016, a dynamic gravity anomaly with a size of 250×125 m and amplitude of -0.022 mGal (more than three times the survey accuracy) was detected. The results of the interpretation have shown that the decrease in the field by 0.02 mGal under a given shape and size of the established dynamic anomaly can be associated with the anomalous body located at a depth of 20 – 50 m (Fig. 10b) whose density has changed by -100 kg/m³. The



Figure 9
Technogenic lake at the location of sinkholes I and II in 2014

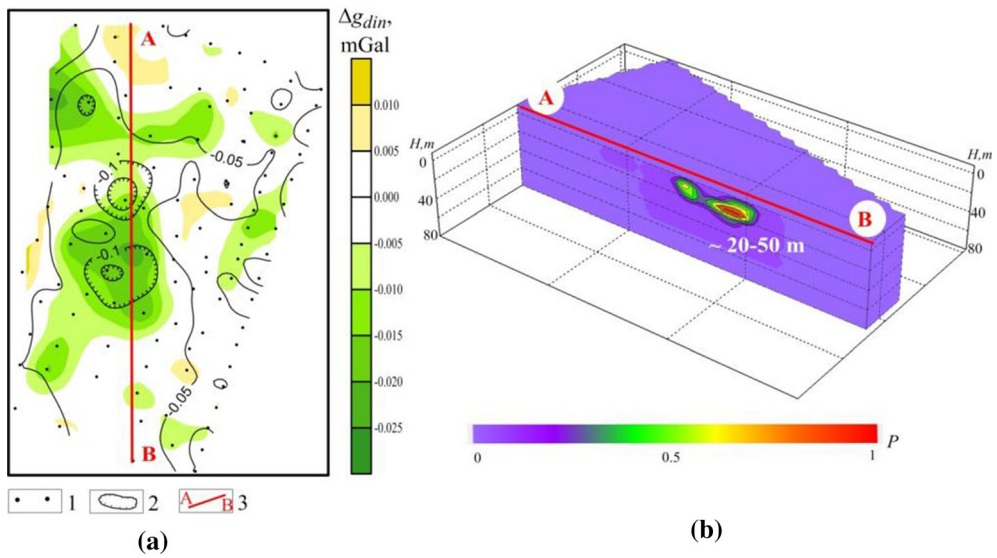


Figure 10

a Dynamic gravity anomaly (September–December 2016) and surface subsidence by September 2017: (1) gravity stations; (2) contour lines of subsidence of the earth’s surface, m; (3) cut line of a 3D chart; **b** the results of gravity inversion for the dynamic anomaly

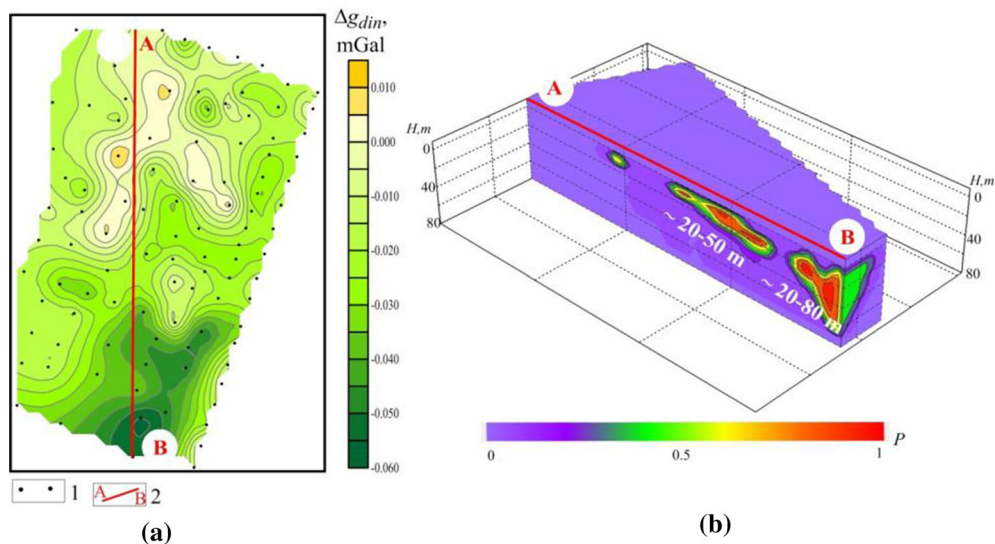


Figure 11

a Dynamic gravity anomaly (September 2017–November 2018): (1) gravity station; (2) cut line of a 3D chart; **b** the results of gravity inversion for the dynamic anomaly

decompaction zone is located in the upper part of the water-resistant stratum. By September 2017, the ground surface within this dynamic anomaly has subsided 15–20 cm.

In November, the epicenter of the dynamic anomaly has moved into the southern part of the study area (Fig. 11a). The amplitude of the anomaly reached -0.06 mGal. At the same time, the depth of the anomalous source remained unchanged -20 – 50 m (Fig. 11b). The decompaction zone creating this dynamic anomaly is, in our opinion, highly hazardous if we consider the fact that it is located in the zone of the negative local gravity anomaly, i.e. in the region of supposed natural decompaction of the rocks. The further gravimetric observations will allow monitoring the dynamics of the processes taking place in the subsurface.

7. Conclusions

Gravimetric studies at the Verkhnekamskoye deposit make certain contribution in studying the density inhomogeneities in the upper part of the section and, hence, in ensuring safety of mining operations and life in the adjacent urbanized area.

The changes in the rock density of the massif under the influence of the mining-geological conditions are clearly recorded in the gravitational field and allow predicting dangerous and catastrophic situations. The methodology for conducting and interpreting the gravimetric monitoring observations, which is presented in this paper, makes it possible to reach a new qualitative level in obtaining information about the distribution and time evolution of density heterogeneities of the geological section, which significantly increases the safety of operation of a mineral deposit.

The suggested technological chain of procedures for interpreting the field data of gravity measurements is based on the successive application of the VECTOR system and the assembly methods, which ensures prompt and highly reliable geological models. In the context of theory, this technology can be considered as an attempt to cope with the ambiguity of the solution of the inverse problem by analyzing the structure of the finite set of the feasible solutions and using a non-traditional approach to selecting the “best” interpretation model. Besides, the technology provides for the possibility of clarifying the vague notions about the rock density parameters of the objects under study. The illustration of the results of

quantitative interpretation in the form of the localization function is, in fact, a visualization of fuzzy sets characterizing the spatial distribution of the studied density heterogeneities. The result of the interpretation is the area of distribution and the probable interval of depths of decompaction of rocks.

Sinkholes of the earth's surface and areas of increased subsidence caused by flooding of mines are clearly recorded in the gravity field. Natural weakened zones are reflected by local negative gravity anomalies. Negative dynamic anomalies indicate the continuation of the process of rock decompaction. By the combination of negative local and dynamic anomalies, it is possible to predict areas of dangerous geological processes.

Acknowledgements

The research was supported by the Russian Foundation for Basic Research (RFBR) (projects no. 19-45-590011 and 19-05-0654).

Publisher's Note Springer Nature remains neutral with regard to jurisdictional claims in published maps and institutional affiliations.

REFERENCES

- Al-Zoubi, A., Eppelbaum, L., Abueladas, A., Ezersky, M., & Akkawi, E. (2013). Removing regional trends in microgravity in complex environments: Testing on 3D model and field investigations in the Eastern Dead Sea Coast (Jordan). *International Journal of Geophysics*. <https://doi.org/10.1155/2013/341797>.
- Arzi, A. A. (1975). Microgravimetry for engineering applications. *Geophysical Prospecting*, 23(3), 408–425. <https://doi.org/10.1111/j.1365-2478.1975.tb01539.x>.
- Bakan, G. M. (2000). Optimization approach to guaranteed state estimation of dynamic systems. *Cybernetics and Systems Analysis*, 36(5), 722–728.
- Balk, P. I., & Dolgal, A. S. (2009). Three-dimensional assembly technologies for the interpretation of gravimetric data. *Doklady Earth Sciences*, 427(2), 971–974. <https://doi.org/10.1134/S1028334X0906018X>.
- Balk, P. I., & Dolgal, A. S. (2010). Deterministic approach to the problem of reliability in interpretation results of gravimetric data. *Doklady Earth Sciences*, 431(1), 334–338. <https://doi.org/10.1134/S1028334X10030153>.
- Balk, P. I., & Dolgal, A. S. (2014). Synthesis of feasible solutions of the inverse problem to prepare recommendations for the verification of gravity anomalies. *Doklady Earth Sciences*, 458(2), 1236–1240. <https://doi.org/10.1134/S1028334X14100018>.
- Balk, P. I., & Dolgal, A. S. (2018). Generalized solutions of the inverse problem and new technologies for the quantitative interpretation of gravity anomalies. *Izvestiya. Physics of the solid Earth*, 54(2), 372–387. <https://doi.org/10.1134/S1069351318020027>.
- Balk, P. I., Dolgal, A. S., & Khristenko, L. A. (2012). Localization of geological objects based on the data of gravity prospecting with incomplete information about the density of rocks. *Doklady Earth Sciences*, 442(2), 262–266. <https://doi.org/10.1134/S1028334X12020122>.
- Baryakh A.A., Sanfirov I.A., Bachurin B.A., Dygilev R.A., Stepanov Y.I. & Bychkov S.G. (2011). Complex researches of the near surface geology effects of the mine-technical collapse. *Environmental Geosciences and Engineering Survey for Territory Protection and Population Safety (EngeoPro-2011)*. Moscow, Russia.
- Biegert, E., Ferguson, J., & Li, X. (2008). 4D gravity monitoring—introduction. *Geophysics*, 73(6), WA1–WA2. <https://doi.org/10.1190/1.3010377>.
- Branston, M. W., & Styles, P. (2003). The application of time-lapse microgravity for the investigation and monitoring of mining subsidence. *Quarterly Journal of Engineering Geology and Hydrogeology*, 36, 231–244. <https://doi.org/10.1144/1470-9236/03-243>.
- Bychkov S. (2018). The tomographic transform of the gravity field and their geological interpretation. *8th Saint Petersburg International Conference & Exhibition*. Saint Petersburg, Russia, 44418. <https://doi.org/10.3997/2214-4609.201800172>.
- Bychkov S., Michurin A. & Simanov A. (2018a). Interpretation of results gravity monitoring of karst processes. *8th Saint Petersburg International Conference & Exhibition*. Saint Petersburg, Russia, 44417. <https://doi.org/10.3997/2214-4609.201800171>.
- Bychkov S.G., Michurin A.V. & Simanov A.A. (2018b). Gravimetric monitoring of technogenic impact on geological environment. *Engineering and Mining Geophysics*. Almaty, Kazakhstan, 46144. <https://doi.org/10.3997/2214-4609.201800459>.
- Bychkov S., Novoselitskiy V., Prostolouпов G., Scherbinina G. & Tchadaev M. (2003). The computer-based system VECTOR as a tool for detection and localization of both gravity and magnetic field sources and its applications at geological interpretation. *Abstracts of Contribution of the EGS-AGU-EUG Joint Assembly*. Nice, France. EAE03-A-01497.
- Bychkov, S. G., Dolgal, A. S., & Simanov, A. A. (2013). Synthesis of qualitative and quantitative methods of extraction of geological information out of gravimetric data. *Eurasian mining*, 2, 12–15.
- Camacho, A. G., Montesinos, F. G., & Vieira, R. (2000). Gravity inversion by means of growing bodies. *Geophysics*, 65(1), 95–101. <https://doi.org/10.1190/1.1444729>.
- Carbone, D., & Greco, F. (2007). Review of microgravity observations at Mt Etna: A powerful tool to monitor and study active volcanoes. *Pure and Applied Geophysics*, 164(4), 769–790. <https://doi.org/10.1007/s00024-007-0194-7>.
- Chapin, D. A., Crawford, M. F., & Baumeister, M. (1999). A side-by-side test of four land gravity meters. *Geophysics*, 64(3), 765–775. <https://doi.org/10.1190/1.1444586>.
- Chernousko, F. L. (1981). Guaranteed ellipsoidal estimates of uncertainties in control problems. *IFAC Proceedings Volumes*,

- 14(2), 869–874. [https://doi.org/10.1016/S1474-6670\(17\)63592-4](https://doi.org/10.1016/S1474-6670(17)63592-4).
- Chianese, D., & Lapenna, V. (2007). Magnetic probability tomography for environmental purposes: Test measurements and field applications. *Journal of Geophysics and Engineering*, 4, 63–74. <https://doi.org/10.1088/1742-2132/4/1/008>.
- Constantino, R. R., Molina, E. C., & de Souza, I. A. (2016). Study of salt structures from gravity and seismic data in Santos Basin. *Brazil. Geofísica Internacional*, 55(3), 199–214. <https://doi.org/10.19155/rgi20165531612>.
- Contrucci, I., Balland, C., Kinscher, J., Bennani, M., Bigarré, P., & Bernard, P. (2019). Aseismic mining subsidence in an abandoned mine: Influence factors and consequences for post-mining risk management. *Pure and Applied Geophysics*, 176(2), 801–825. <https://doi.org/10.1007/s00024-018-2015-6>.
- Davis, K., Li, Y., & Batzle, M. (2008). Time-lapse gravity monitoring: A systematic 4D approach with application to aquifer storage and recovery. *Geophysics*, 73(6), WA61–WA69. <https://doi.org/10.1190/1.2987376>.
- Dolgal, A. S., Bychkov, S. G., Kostitsyn, V. I., Novikova, P. N., Pugin, A. V., Rashidov, V. A., & Sharkhimullin, A. F. (2012). On the theory and practice of the tomographic interpretation of geopotential fields. *Geophysics*, 5, 8–17. (in Russian).
- Eppelbaum, L. V., Ezersky, M., Al-Zoubi, A., Goldshmidt, V., & Legchenko, A. (2008). Study of the factors affecting the karst volume assessment in the Dead Sea sinkhole problem using microgravity field analysis and 3-D modelling. *Advances in GeoSciences*, 19, 97–115. <https://doi.org/10.5194/adgeo-19-97-2008>.
- Florio, G., & Fedi, M. (2014). Multiridge euler deconvolution. *Geophysical Prospecting*, 62(2), 333–351. <https://doi.org/10.1111/1365-2478.12078>.
- Gabriel G., Kobe M., Weise A., & Timmen L. (2019). Monitoring of Subrosion Induced Mass Changes by Time-Lapse Gravity Surveys – Two Case Studies from Germany. *Near Surface Geoscience Conference & Exhibition 2019*. The Hague, Netherlands. Mo_25th_B10. <https://doi.org/10.3997/2214-4609.201902587>.
- Gasperikova, E., & Hoversten, G. M. (2008). Gravity monitoring of CO₂ movement during sequestration: Model studies. *Geophysics*, 73(6), WA105–WA112. <https://doi.org/10.1190/1.2985823>.
- Gelderen, M., Haagmans, R., & Bilker, M. (1999). Gravity changes and natural gas extraction in Groningen. *Geophysical Prospecting*, 47(6), 979–993. <https://doi.org/10.1046/j.1365-2478.1999.00159.x>.
- Glegola, M., Ditmar, P., Vossepoel, F., Arts, R., Al-Kindy, F., & Klees, R. (2015). Gravimetric monitoring of the first field-wide steam injection in a fractured carbonate field in Oman—a feasibility study. *Geophysical Prospecting*, 63(5), 1256–1271. <https://doi.org/10.1111/1365-2478.12150>.
- Jacob, T., Chery, J., Bayer, R., Moigne, N. L., Boy, J.-P., Vernant, P., & Boudin, F. (2009). Time-lapse surface to depth gravity measurements on a karst system reveal the dominant role of the epikarst as a water storage entity. *Geophysical Journal International*, 177(2), 347–360. <https://doi.org/10.1111/j.1365-246X.2009.04118.x>.
- Jacoby, W., & Smilde, P. (2009). *Gravity interpretation*. Springer, Berlin Heidelberg: Fundamentals and Application of Gravity Inversion and Geological Interpretation.
- Jentsch, G., Weise, A., Rey, C., & Gerstenecker, C. (2004). Gravity changes and internal processes: Some results obtained from observations at three volcanoes. *Pure and Applied Geophysics*, 161(7), 1415–1431. <https://doi.org/10.1007/s00024-004-2512-7>.
- Kovin, O. (2011). Mapping of evaporite deformation in a potash mine using ground penetrating radar: Upper kama deposit, Russia. *Journal of Applied Geophysics*, 74, 131–141. <https://doi.org/10.1016/j.jappgeo.2011.04.009>.
- Liu, G., Yanb, H., Meng, X., & Chen, Z. (2014). An extension of gravity probability tomography imaging. *Journal of Applied Geophysics*, 102, 62–67. <https://doi.org/10.1016/j.jappgeo.2013.12.012>.
- Mauriello, P., & Patella, D. (2001). Gravity probability tomography: A new tool for buried mass distribution imaging. *Geophysical Prospecting*, 49(1), 1–12. <https://doi.org/10.1046/j.1365-2478.2001.00234.x>.
- Nava-Flores, M., Ortiz-Aleman, C., Orozco-del-Castillo, M. G., Urrutia-Fucugauchi, J., Rodriguez-Castellanos, A., Couder-Castañeda, C., & Trujillo-Alcantara, A. (2016). 3D Gravity modeling of complex salt features in the Southern Gulf of Mexico. *International Journal of Geophysics*. <https://doi.org/10.1155/2016/1702164>.
- Novoselitskiy V., Prostoloupov G., Scherbinina G., Iakovlev S. & Bychkov S. (2003). Microgravity investigation for solution an engineering and geological problems by use the computer-based system «VECTOR». *International workshop «Geosciences for urban development and environmental plating»*, (pp. 118–120). Vilnius, Lithuania.
- Ogilvy, A. A., & Bogoslovsky, V. A. (1979). The possibilities of geophysical methods applied for investigating the impact of man on the geological medium. *Geophysical Prospecting*, 27(4), 775–789. <https://doi.org/10.1111/j.1365-2478.1979.tb00996.x>.
- Pinto, V., Casas, A., Rivero, L., & Torné, M. (2005). 3D gravity modeling of the Triassic salt diapirs of the Cubeta Alavesa (northern Spain). *Tectonophysics*, 405(1), 65–75. <https://doi.org/10.1016/j.tecto.2005.05.010>.
- Pringle, J. K., Styles, P., Howell, C. P., Branston, M. W., Furner, R., & Toon, S. M. (2012). Long term time lapse microgravity and geotechnical monitoring of relict salt mines Marston Cheshire U K. *Geophysics*, 77(6), B287–B294. <https://doi.org/10.1190/GEO2011-0491.1>.
- Prostoloupov, G. V., Novoselitskiy, V. M., Koneshov, V. N., & Shcherbinina, G. P. (2006). Gravity and magnetic field interpretation based on transformations of horizontal gradients in the VECTOR system. *Izvestiya, Physics of the Solid Earth*, 42(6), 530–535. <https://doi.org/10.1134/S1069351306060103>.
- Reitz, A., Krahenbuhl, R., & Li, Y. (2015). Feasibility of time-lapse gravity and gravity gradiometry monitoring for steam-assisted gravity drainage reservoirs. *Geophysics*, 80(2), WA99–WA110. <https://doi.org/10.1190/geo2014-0217.1>.
- Rybakov, M., Goldshmidt, V., Fleischer, L., & Rotstein, Y. (2001). Cave detection and 4-D monitoring: A microgravity case history near the Dead Sea. *The Leading Edge*, 20(8), 896–900. <https://doi.org/10.1190/1.1487303>.
- Sailhac, P., Gibert, D., & Boukerbout, H. (2009). The theory of the continuous wavelet transform in the interpretation of potential fields: A review. *Geophysical Prospecting*, 57(4), 517–525. <https://doi.org/10.1111/j.1365-2478.2009.00794.x>.
- Santolaria, P., Casas-Sainz, A. M., Soto, R., & Casas, A. (2017). Gravity modeling to assess salt tectonics in the western end of the South Pyrenean Central Unit. *Journal of the Geological Society*, 174(2), 269–288. <https://doi.org/10.1144/jgs2016-027>.

- Shcherbinina, G. P., Prostolupov, G. V., & Bychkov, S. G. (2011). The gravimetrical survey in handling the geological and mining problems at the Upper Kama potassium salt deposit. *Journal of Mining Science*, 47(5), 566–572. <https://doi.org/10.1134/S1062739147050042>.
- Strakhov, V. N., & Lapina, M. I. (1976). Mounting method for solving the inverse problem of gravimetry. *Reports of the Academy of Sciences of the USSR*, 227(2), 344–347. (in Russian).
- Strzałkowski, P. (2019). Some remarks on impact of mining based on an example of building deformation and damage caused by mining in conditions of upper Silesian coal basin. *Pure and Applied Geophysics*, 176(6), 2595–2605. <https://doi.org/10.1007/s00024-019-02127-1/>.
- Styles, P., Toon, S., Thomas, E., & Skittrall, M. (2006). Micro-gravity as a tool for the detection, characterization and prediction of geohazard posed by abandoned mining cavities. *First Break*, 24, 51–60. <https://doi.org/10.3997/1365-2397.2006013>.
- Sultan, M., & Ahmed, K. A. (2014). Composite geophysical study comprising gravity, magnetic, and resistivity surveys to delineate basement salt deposits near Jabbar Nala East of Kherwa Gorge Pakistan. *Journal of Geology & Geophysics*. <https://doi.org/10.4172/2329-6755.1000182>.
- Tsiupiak A. I., Anikeyev S. G., & Hablovskiy B. B. (2019) Gravitational monitoring substantiation by imitation modelling methods. *18th EAGE International Conference on Geoinformatics-Theoretical and Applied Aspects*. Kyiv, Ukraine. <https://doi.org/10.3997/2214-4609.201902040>
- Xiao, F. (2015). Gravity correlation imaging with a moving data window. *Journal of Applied Geophysics*, 112, 29–32. <https://doi.org/10.1016/j.jappgeo.2014.11.004>.
- Zong, J., Coskun, S., Stewart, R. R., Dyaour, N., & Myers, M. T. (2015). *Salt densities and velocities with application to Gulf of Mexico salt domes*. New Orleans: SEG Annual Meeting Post-convention Workshop.

(Received March 13, 2020, revised December 1, 2020, accepted December 3, 2020, Published online January 8, 2021)